Evolution of the additive genetic variance-covariance matrix under continuous directional selection on a complex behavioral phenotype

Vincent Careau[1], Matthew E. Wolak[2], Patrick A. Carter[3], Theodore Garland, Jr.[4]

[1]Canada Research Chair in Functional Ecology, Department of Biology, University of Ottawa, Ottawa, ON, Canada

[2]School of Biological Sciences, University of Aberdeen, Aberdeen, UK

[3]School of Biological Sciences, Washington State University, Pullman, WA, USA

[4]Department of Biology, University of California, Riverside, CA, USA

Author for correspondence:

Vincent Careau (vcareau@uottawa.ca)

Electronic Supplemental Material

Table of Contents

Table S1. Sample sizes. Number of individuals (and families) measured for their voluntary wheel running over a 6-days period in control (C) and high-runner (HR) lines of mice, for the entire dataset (generations 0 to 31) and different periods.

Generation	C	HR	Total
0 to 10			
Individuals	1,687	4,493	6,180
Families	443	441	884
11 to 20			
Individuals	1,569	3,740	5,309
Families	400	397	797
21 to 31			
Individuals	1,680	4,159	5,839
Families	432	432	864
0 to 31			
Individuals	4,936	12,392	17,328
Families	1,275	1,270	2,545

Table S2. Summary of the genetic covariance tensor applied to the 24 **G** matrices estimated for each of the 8 lines and 3 generation blocks. Shown are the eigenvectors (***e***; ordered by rows in terms of the absolute value) of the two leading eigentensors ($\mathbf{E}_1$ and $\mathbf{E}_2$), their eigenvalues and the percent of variation each eigentensor explains within their respective **E**, and loadings on each trait (wheel running on days 1 to 6). This table shows that the leading eigentensor ($\mathbf{E}_1$) captured a large part (75.6%) of the variance among **G** matrices and that the leading eigenvector $\boldsymbol{e}_{11}$ explained 99.6% of the variation captured by $\mathbf{E}_1$, with loadings ranging from -0.35 to -0.45 only. Applying the tensor analysis to the 24 **G** matrices estimated for each line and generation block yielded results that are consistent with the analysis in which control and selected lines are pooled (see table 1).

Eigentensors (**E**)	Eigenvalues of **E**	% of total variation explained	Eigenvectors (***e***) of **E**	Eigenvalues of ***e***	% of variation explained in **E**	Trait loadings					
						day 1	day 2	day 3	day 4	day 5	day 6
$\mathbf{E}_1$	0.2793	76.5%	$e_{1.1}$	-0.998	99.6%	-0.348	-0.401	-0.400	-0.435	-0.448	-0.410
			$e_{1.2}$	-0.046	0.2%	0.753	0.305	0.018	-0.147	-0.289	-0.485
			$e_{1.3}$	-0.034	0.1%	0.444	-0.286	-0.336	-0.536	0.279	0.493
			$e_{1.4}$	-0.021	0.0%	0.063	0.209	-0.829	0.505	-0.060	0.082
			$e_{1.5}$	-0.018	0.0%	-0.295	0.762	-0.067	-0.458	-0.202	0.278
			$e_{1.6}$	-0.013	0.0%	0.154	-0.200	0.187	0.195	-0.771	0.519
$\mathbf{E}_2$	0.0279	7.7%	$e_{2.1}$	0.711	50.5%	-0.788	-0.524	-0.263	-0.178	-0.067	-0.020
			$e_{2.2}$	-0.703	49.5%	0.289	-0.055	-0.292	-0.402	-0.578	-0.577
			$e_{2.3}$	-0.020	0.0%	0.267	-0.269	0.136	-0.779	0.439	0.194
			$e_{2.4}$	0.012	0.0%	-0.170	0.171	0.475	-0.272	-0.637	0.486
			$e_{2.5}$	-0.002	0.0%	0.413	-0.774	0.108	0.351	-0.228	0.209
			$e_{2.6}$	0.000	0.0%	0.160	0.150	-0.768	-0.043	-0.106	0.591

Table S3. Vector of realized selection gradients (β) applied to voluntary wheel running on each day of a 6-day period of wheel access. Posterior modes with their 95% highest posterior density (HPD) intervals obtained from a multiple regression of relative fitness (number of pups produced) were obtained using different blocks of generations. The target of selection was the average number of wheel revolutions on days 5&6. Boldface highlights selection gradients that were significantly different from zero (i.e., the 95% HPD did not overlap with zero). Note that some selection gradients on days 1 to 4 were negative and significantly different from zero.

generation			95% HPD	
block	trait	β	lower	upper
0-10	day 1	**-0.077**	**-0.152**	**-0.026**
0-10	day 2	**-0.092**	**-0.171**	**-0.017**
0-10	day 3	0.010	-0.068	0.094
0-10	day 4	-0.064	-0.154	0.008
0-10	day 5	**0.758**	**0.668**	**0.847**
0-10	day 6	**0.528**	**0.445**	**0.625**
11-20	day 1	-0.024	-0.111	0.038
11-20	day 2	0.003	-0.103	0.083
11-20	day 3	-0.018	-0.104	0.078
11-20	day 4	**-0.111**	**-0.230**	**-0.033**
11-20	day 5	**0.457**	**0.352**	**0.569**
11-20	day 6	**0.721**	**0.611**	**0.802**
21-31	day 1	**-0.072**	**-0.158**	**0.006**
21-31	day 2	0.065	-0.038	0.175
21-31	day 3	**-0.127**	**-0.239**	**-0.022**
21-31	day 4	-0.003	-0.136	0.096
21-31	day 5	**0.481**	**0.333**	**0.568**
21-31	day 6	**0.542**	**0.411**	**0.611**

Table S4. Predicted response to selection (**R**). Posterior modes and 95% highest posterior density (HPD) intervals for the six behavioural traits in control (C) and selected (HR; for "high runner") mice in different blocks of generations. To obtain the posterior distribution of **R** that incorporates the uncertainty in estimates of both **G** and β, we applied the multivariate breeder's equation to the i^{th} sample of the MCMC posterior distribution for **G** with the i^{th} sample of the MCMC posterior distribution for β (table S2). These calculations were made separately for each generation block (i.e., using the six **G**-matrices in figure S3 and the 3 β in table S3). This table demonstrates that the predicted response to selection was ~4-fold lower in HR than C mice, but that the **R** for days 5&6 in generations 21-31 was still significantly different from zero, even for HR mice.

generation		C			HR		
block	trait	**R**	lower	upper	**R**	lower	upper
0-10	day 1	0.13	0.06	0.21	0.04	0.01	0.06
0-10	day 2	0.15	0.08	0.24	0.04	0.02	0.08
0-10	day 3	0.15	0.08	0.25	0.04	0.01	0.07
0-10	day 4	0.16	0.09	0.27	0.03	0.02	0.07
0-10	day 5	0.20	0.14	0.32	0.06	0.03	0.08
0-10	day 6	0.24	0.14	0.33	0.06	0.04	0.10
11-20	day 1	0.17	0.08	0.25	0.02	0.00	0.05
11-20	day 2	0.13	0.08	0.24	0.03	0.01	0.05
11-20	day 3	0.14	0.06	0.23	0.02	0.00	0.05
11-20	day 4	0.18	0.10	0.28	0.04	0.02	0.08
11-20	day 5	0.19	0.13	0.32	0.06	0.04	0.09
11-20	day 6	0.18	0.10	0.26	0.06	0.04	0.08
21-31	day 1	0.14	0.08	0.22	0.03	0.00	0.06
21-31	day 2	0.18	0.11	0.27	0.03	0.01	0.06
21-31	day 3	0.17	0.11	0.27	0.03	0.01	0.06
21-31	day 4	0.19	0.11	0.28	0.04	0.01	0.07
21-31	day 5	0.24	0.15	0.34	0.05	0.03	0.09
21-31	day 6	0.24	0.15	0.33	0.05	0.03	0.08

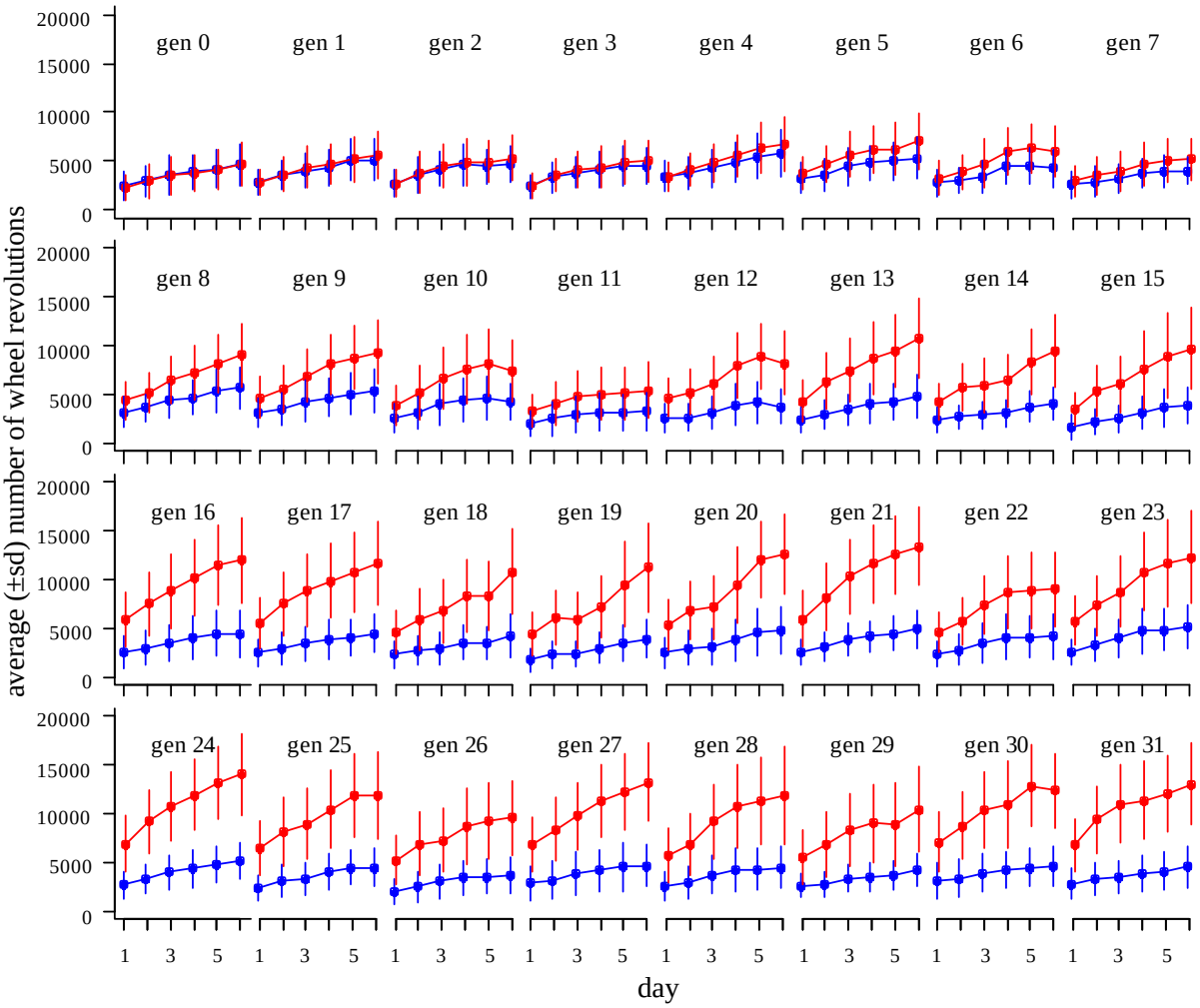

Figure S1. Daily and generational increases in wheel running in mice. Shown are the daily average number of wheel revolutions run (pooled means±sd [ignoring family structure] for four replicate lines in each selection group) over a 6-day period of wheel access in four replicate control (C; blue) and four replicate selected (HR, for “high runners”; red) mice over a 6-day period of wheel access, from generation 0 (before any selection was applied) to 31.

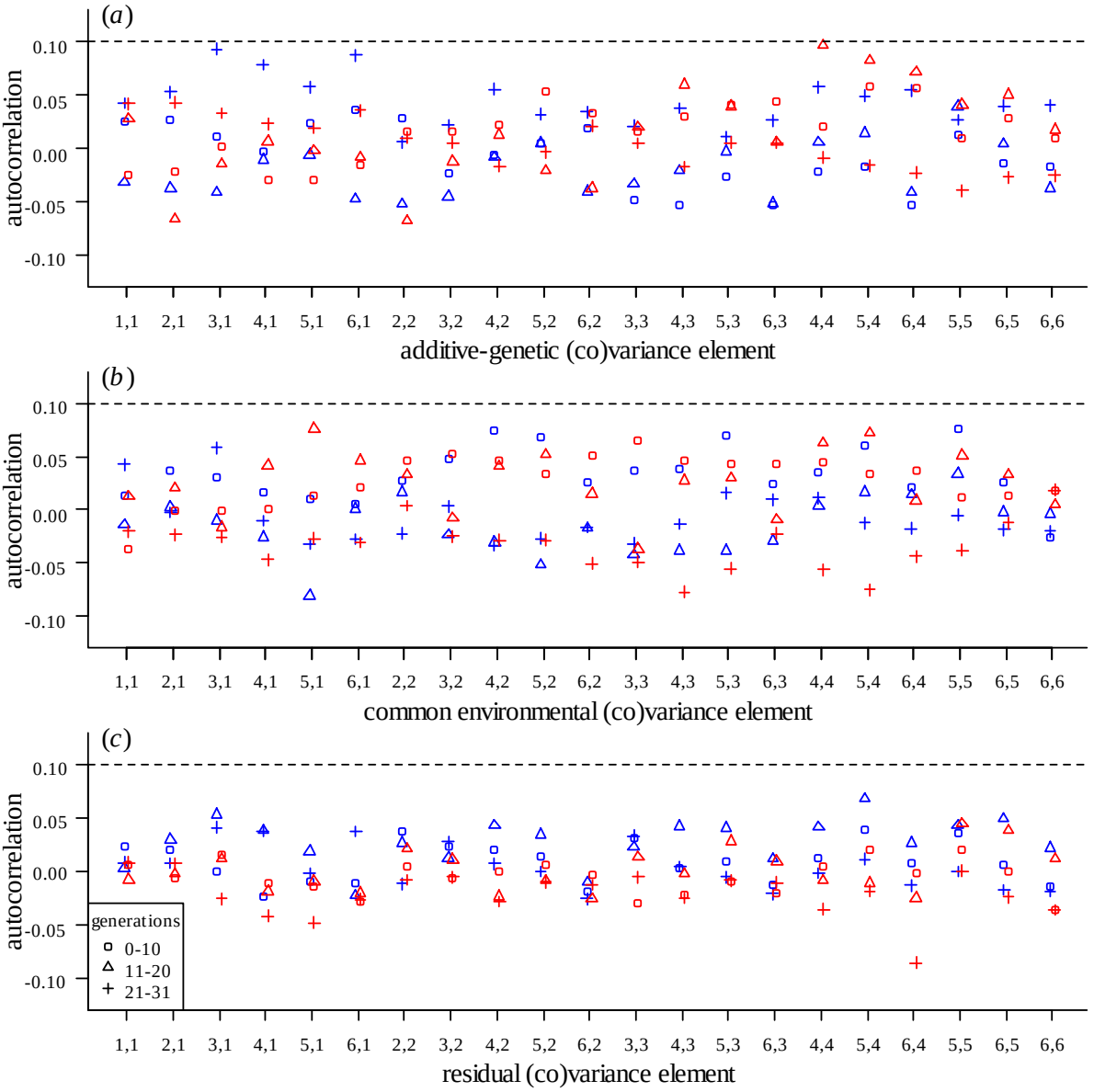

Figure S2. Convergence for MCMCglmm models. (*a*-*c*) Autocorrelation (i.e., at lag 1) of the 1,000 posterior samples for each of the estimated variance components in multivariate animal models run on pooled data for control (blue) and selected (red) mice for different generation blocks. No (co)variance component exceeded the nominal autocorrelation of 0.1. These diagnostic plots indicate that the MCMCglmm models converged properly.

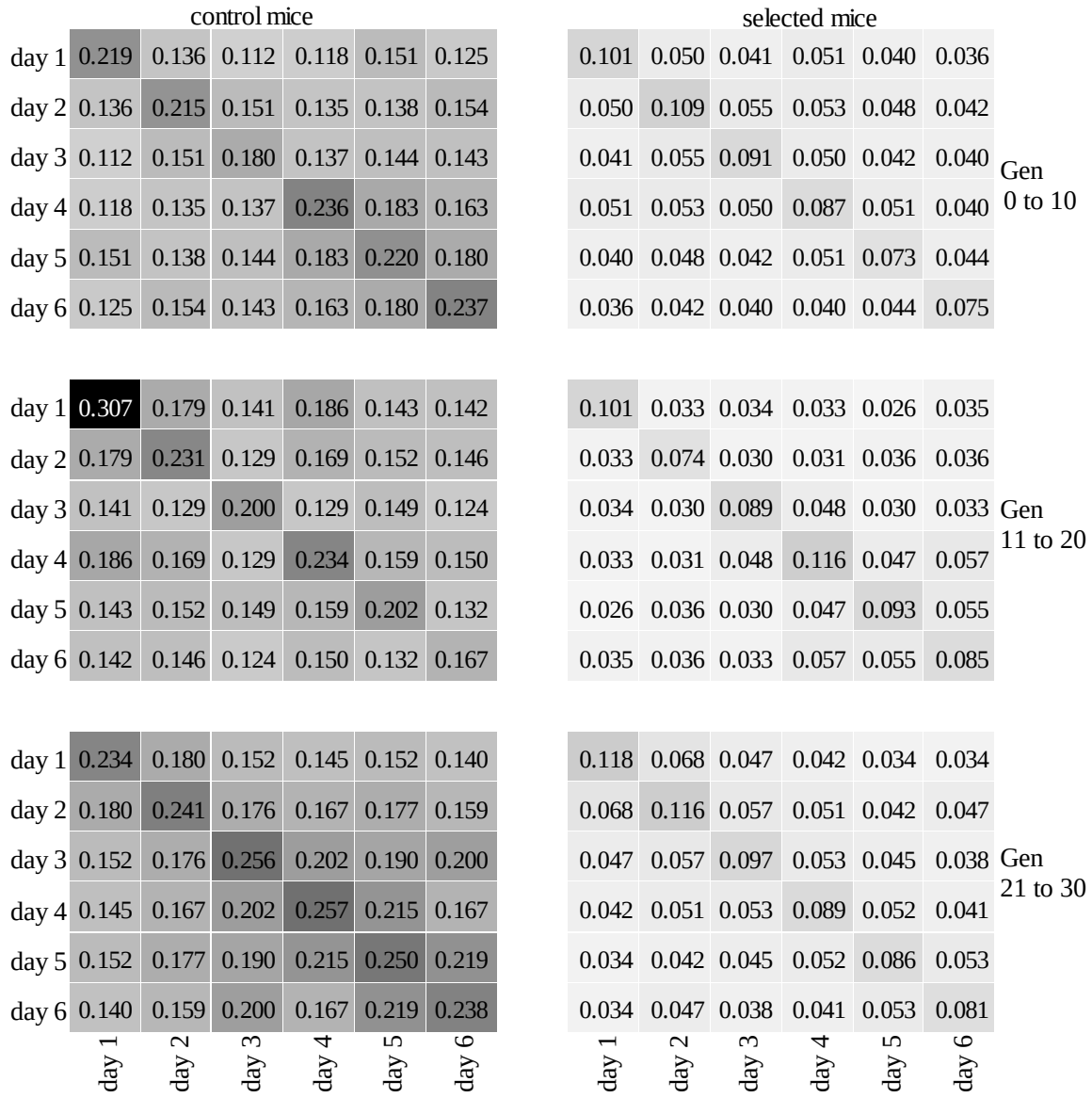

Figure S3. The estimated additive-genetic variance-covariance matrices (**G**) in control and selected mice, based on pooled analyses of all 4 replicate lines in each group). Shown are the posterior modes from Bayesian multivariate animal models fitted with MCMCglmm in R on different blocks of generations (0 to 10, 11 to 20, and 21 to 31). For each **G**, the main diagonal represents the additive-genetic variances (V_A) and the off-diagonals represent the additive-genetic covariances (COV_A) for pairs of traits (voluntary wheel running on each of 6 consecutive days). The cells of the matrix are shaded according to its value (darker cell = higher V_A or COV_A: all values are positive). (See figure S4*d-f* for the genetic correlations.)

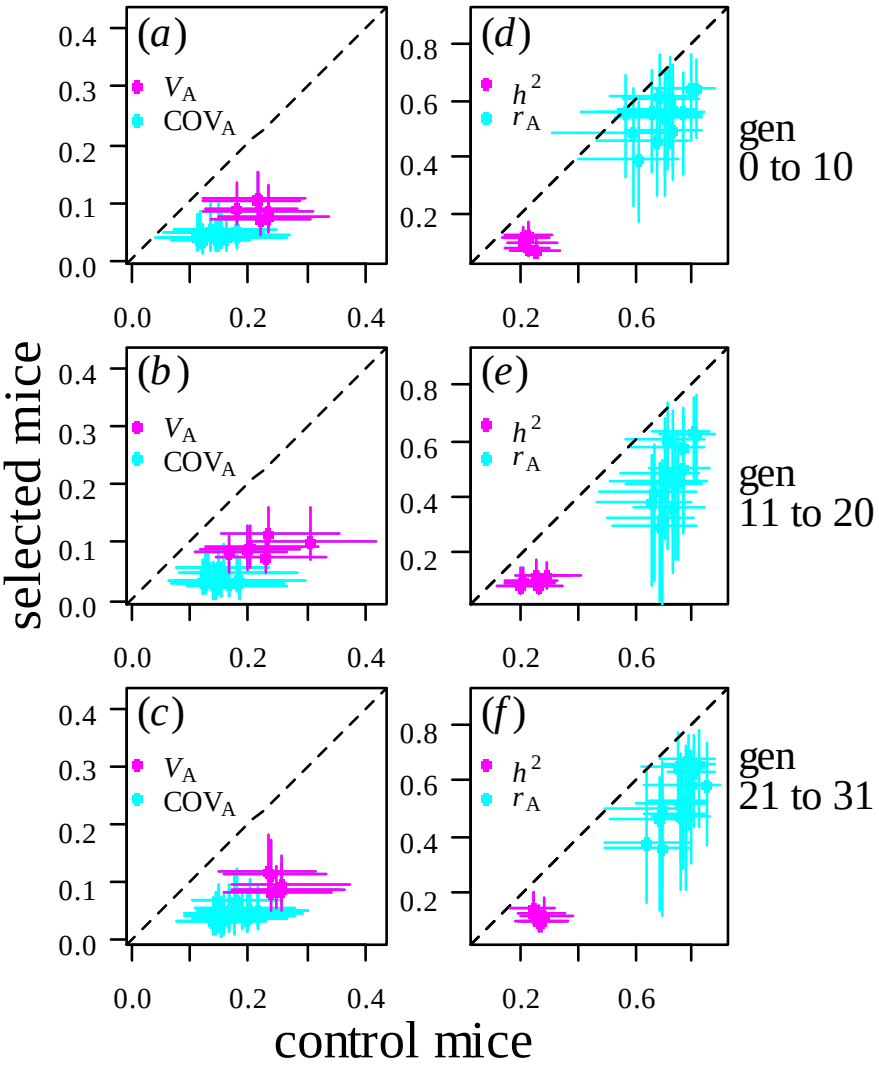

Figure S4. Elements of the additive-genetic variance-covariance matrices. (*a-c*) The posterior modes (dots) and 95% credible intervals (lines) of the highest posterior density from Bayesian multivariate animal models fitted with MCMCglmm in R on different blocks of generations (0 to 10, 11 to 20, and 21 to 31). Each point represents the same element of the matrix [additive-genetic variance (V_A) and co-variance (COV_A)] in selected mice (on the *y* axis) vs. control mice (on the *x* axis). The dashed line shows the 1:1 line. Note that compared to control, selected mice always have lower V_A for all 6 days of wheel running, and weaker positive COV_A among those traits. (*d-f*) Also shown are the corresponding narrow-sense heritability (h^2) and genetic correlations (r_A).

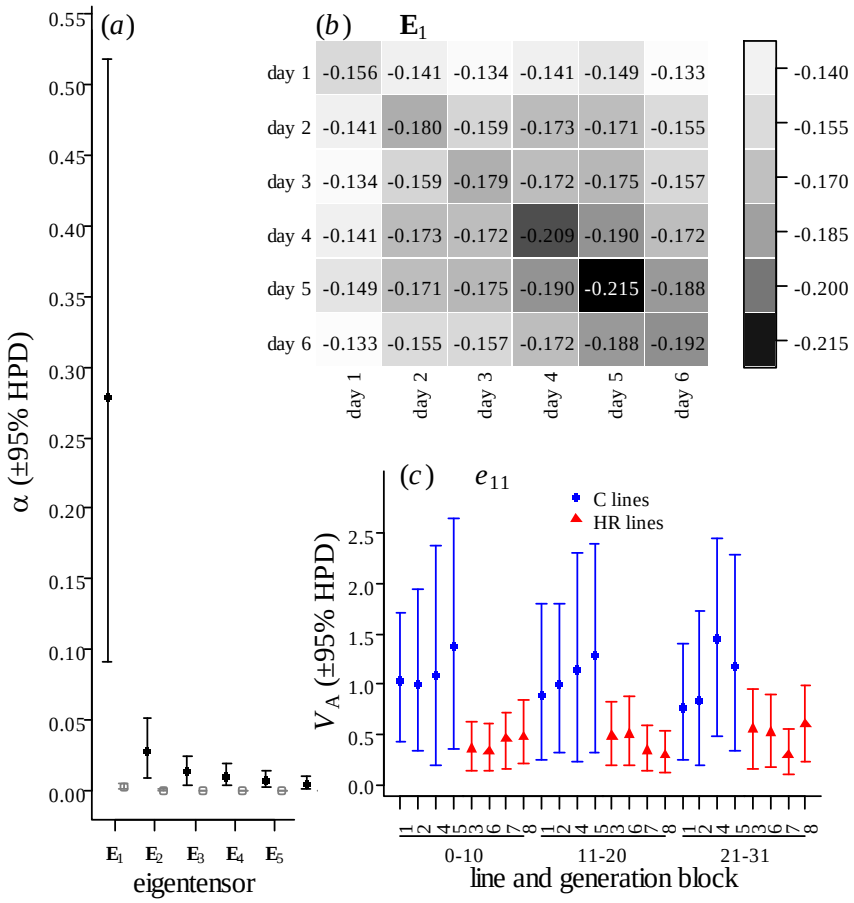

Figure S5. Changes in the additive-genetic variance-covariance matrix (**G**) induced by selection, presented at the level of replicate lines (control lines: 1, 2, 4, and 5; selected line: 3, 6, 7, and 8). (*a*) Variance [α; ±95% highest posterior density (HPD) intervals] accounted for by each eigentensor for the observed (black dots) and randomized (i.e., null hypothesis; grey dots) sets of **G**. (*b*) "Heat map" displaying the pattern of greatest variation among **G**s as captured by $\mathbf{E}_1$ (darker shading indicates greater variation among **G** matrices as measured by elements of $\mathbf{E}_1$, which reflect variance of the (co)variances among the 6 **G** matrices). Hence, variability among **G** matrices was distributed throughout the entire matrix, but slightly more intense for trait combinations involving days 4-6 compared to those earlier in the day sequence. (*c*) The additive-genetic variance (V_A) present in each of the four replicate control lines (C; blue) and four replicate selected lines (HR; red) along the direction of the first eigenvector of $\mathbf{E}_1$ (i.e., $\boldsymbol{e}_{11}$) across generation blocks. Altogether, this figure shows that the effect of selection on **G** was repeatable and that variance among **G** matrices was not caused solely by random genetic drift.

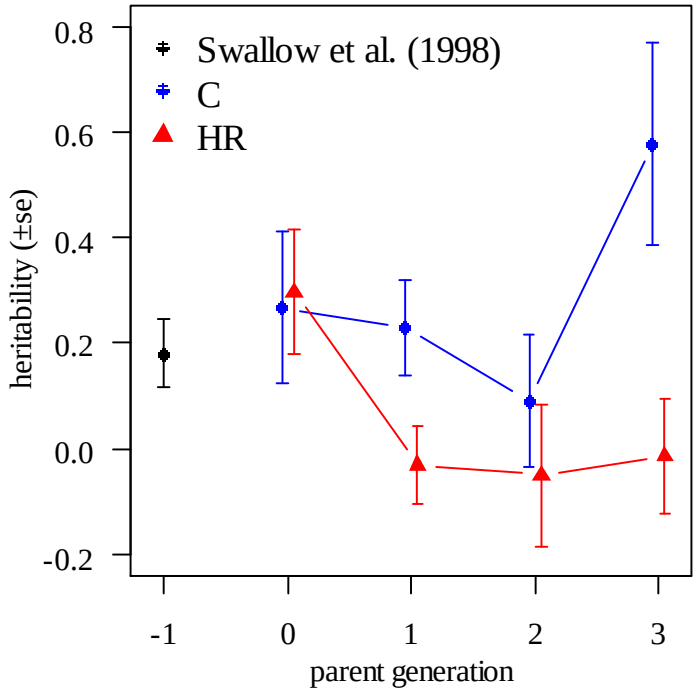

Figure S6. Heritability (±se) of voluntary wheel running on days 5&6 (the selected trait) estimated with offspring-on-midparent regressions in generation -1 and 0 by Swallow et al. (Behav. Genet. 28: 227-237) and in control (C; blue dots) and selected (HR; red triangles) mice using data from generation 0 to 1, 1 to 2, 2 to 3, and 3 to 4. For C and HR mice separately, we first calculated residual values in a model that included several fixed effects fit within generation [sex, age, inbreeding coefficient, line, and measurement block (batches 1-3 and rooms 1-2)]. The residuals of these models were then used in regressions weighted for litter size using an iterative process as described in Lynch and Walsh (1998, Genetics and Analysis of Quantitative traits, p541), using the "osw.R" function accompanying Careau *et al.* (2013, Evolution 67: 3102-3119). The weight (w_i) of the i^{th} family was calculated as $w_i=n_i/[n_i(t–B)+(1–t)]$, where n_i is the number of mice that were wheel-tested in that family, t the intraclass correlation coefficient (for that line at that generation), and B is the slope squared divided by two. This figure shows that heritability of wheel running was initially similar in C and HR mice, but rapidly declined in HR mice.

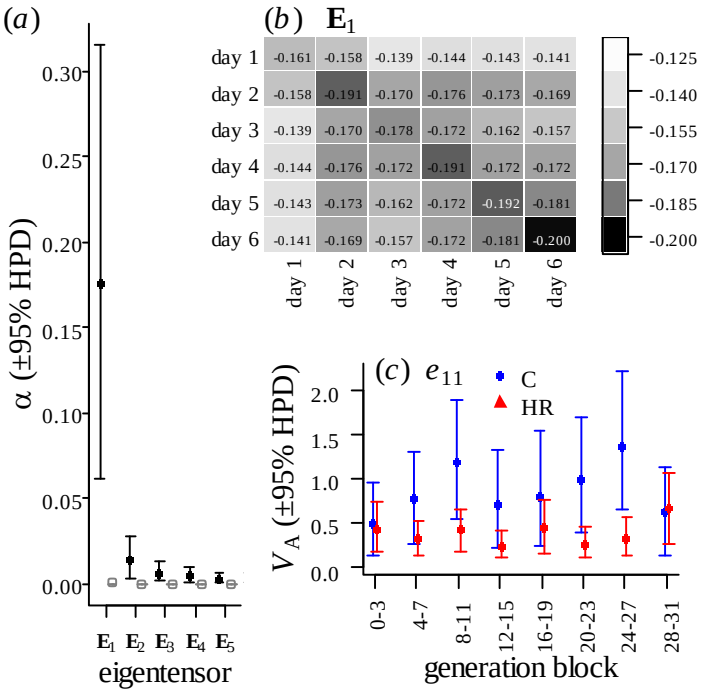

Figure S7. Changes in the additive-genetic variance-covariance matrix (**G**) induced by selection, presented as in Figure 2 (main text; see also figure S5 above), except that the genetic covariance tensor was applied to blocks of 4 generations in control (C) and selected (HR) mice. Altogether, this figure shows that V_A along $\boldsymbol{e}_{11}$ was similar in C and HR mice at the beginning of the experiment (generation 0-3), after which C and HR mice gradually diverged. Note that for this analysis, the sample size to estimate **G** was quite low (C mice: mean n = 617, range = 596-649; HR mice: mean n = 1,619, range = 1,405-1,631).

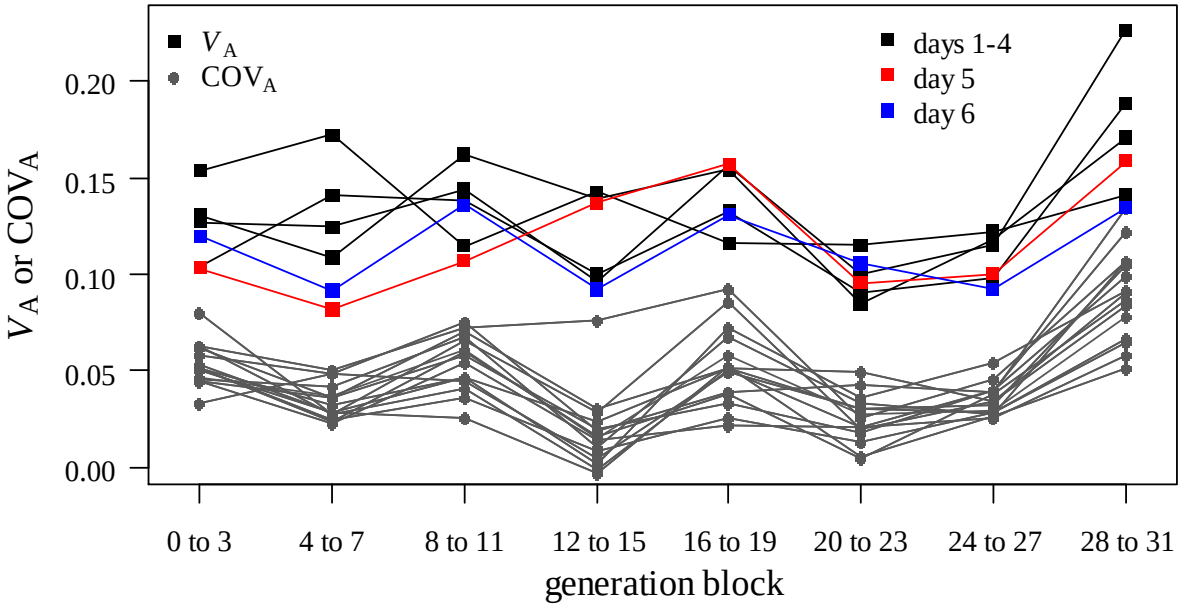

Figure S8. Absence of detectable change in the additive-genetic variance-covariance matrix (**G**) in selected mice, based on pooled analyses of all 4 lines. This shows each element of **G** [i.e., additive-genetic variance (V_A) in wheel running on days 1-4 (black squares), day 5 (red square), day 6 (blue square), and the additive-genetic covariances (COV_A) among all six traits (grey circles)] in mice selected for voluntary wheel running on days 5&6 of a 6-day exposure to wheels, as estimated in separate MCMCglmm models run on blocks of 4 generations. Note the absence of overall temporal change, thus indicating that the effect of selection on **G** occurred very rapidly (i.e., within the first three generations). Repeating these analyses, but breaking up the estimation of **G** into even smaller blocks (i.e., 2 or 3 generations), suffered from an obvious lack of statistical power to detect changes within the first 2-3 generations of selection.

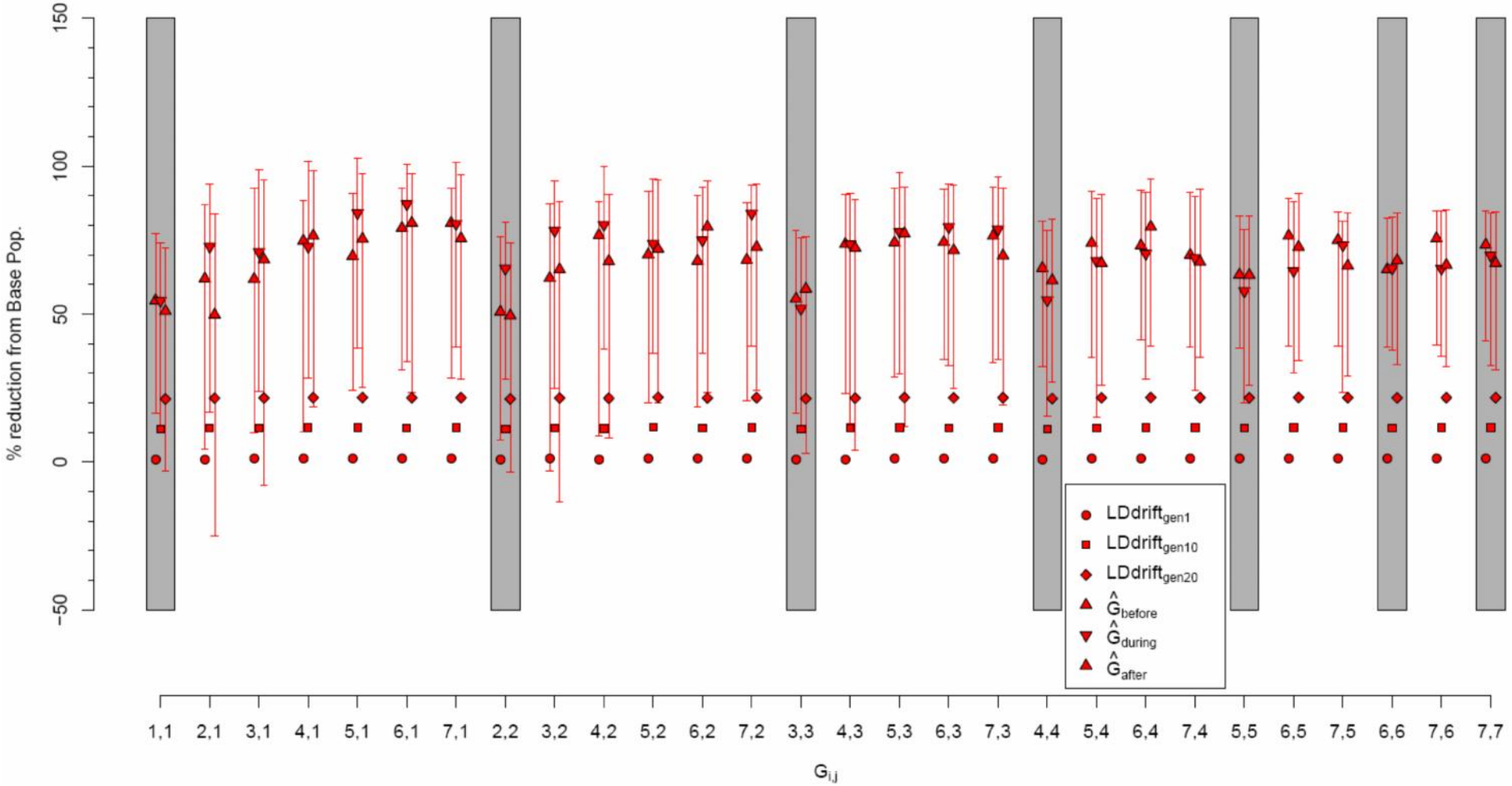

Figure S9: Observed and predicted percent reductions in each element of the additive-genetic variance-covariance matrix **G** for wheel running on days 1-6 in mice selected for voluntary wheel running on days 5&6 of a 6-day exposure to wheels. Values are the % reduction from the base population **G** matrix (estimated for the base stock of mice used to found the control and selected lines, using generations -2, -1, and 0) in each element of the lower triangle of the observed **G** from the MCMCglmm models in the before (up-pointing triangle that is the left-most point of each trio of triangles), during (down-pointing triangle), and after (up-pointing triangle that is the right-most point of each trio of triangles) generation blocks along with their 95% HPD intervals. The % reduction was calculated as [100 × (observed **G** – base **G**) / base **G**]. The expected **G** matrices were calculated based on within-family selection operating on an index trait (average of days 5&6) in the base population **G** matrix and changes occurring through linkage disequilibrium (LD; Bulmer, 1980, The mathematical theory of quantitative genetics. Oxford University Press, Oxford, UK) and drift (or inbreeding within each selection line). The expected **G** used in place of the observed **G** in the percent reduction equation were calculated for 1 (circles), 10 (squares), and 20 (diamonds) generations to match the observed **G** estimated in the three corresponding generation blocks. Grey, rectangular background shading indicates the diagonal elements of **G** (i.e., V_A) for reference. Overall, this figure demonstrates that the predicted changes in the (co)variance components due to selection generating LD are much lower than the observed changes in the selected mice. Details on the theory and calculations are available from the authors and various references (Falconer & MacKay, 1996, Introduction to Quantitative Genetics, 4th ed. Essex, U.K.: Longman; 1996; Shaw *et al*., 1995, Evolution 49: 1260-1267; Verrier *et al*., 1991, Livestock Production Science 29: 93-114; Villanueva and Kennedy 1990. Theoretical and Applied Genetics 80: 746-752).

Appendix S1: Establishment of experimental lines

Details regarding the establishment and maintenance of the control and selected lines can be found in previous publications (Swallow *et al.* 1998. Behav. Genet. 28: 227-237; Careau *et al.* 2013. Evolution 67: 3102-3119). Only the pertinent details are repeated here for clarity. A total of 112 male and 112 female (each specified to be from a different family) house mice (*Mus domesticus*) of the Hsd:ICR strain were purchased from Harlan Sprague Dawley, Indianapolis, IN (Building 202, Barrier A). The history and maintenance of the Hsd:ICR strain can be found in Swallow *et al.* (1998), Dohm *et al.* (2001. Genetics 159: 267-277), and Girard *et al.* (2002. Behav. Proces. 57: 37-50).

The 224 founder animals were designated generation -2. Males and females were chosen at random and placed into cages to form 112 pairs; the resulting offspring were designated generation -1. Generation -1 litters were randomly assigned to one of eight lines, and one male and one female were chosen randomly from each litter to be breeders for that line. Individuals within each line that had been chosen to be breeders were then paired randomly except that full-sibling mating was disallowed; 10 pairs were established for each line (plus 3 additional pairs as backups: see below). Lines were then randomly assigned into four non-selected control (C) lines and four selected "high-runner" (HR) lines. Their offspring were designated generation 0 and selection was first applied at this generation in HR lines. In each of the 4 HR lines, the male and female from each family that was ranked highest according to the selection criteria (see main text) were randomly paired with individuals from other families in that same line, avoiding full-sibling matings. In C lines, one male and one female were chosen at random from each family and randomly paired, avoiding full-sibling matings. For most generations, 13 pairs were established within each line where the first 10 litters weaned with at least two pups of each sex

were used to maintain that line. The three extra families per line were backups to ensure that each line was propagated with 10 families per generation.

Breeder mice were paired at approximately 10 weeks of age (except generation -2, which was paired at 7 weeks, and generations -1 and 0, which were paired at 8.5 weeks of age) by placing one male and one female together in a fresh cage. Males were removed and weighed 15-18 days after pairing; births began 19 days after pairing. From 19 to 33 days after pairing, pregnant females were checked daily between 1600 and 1800. On the day of parturition, the number of pups was recorded. At 21 days of age, offspring were weaned from the dam, weighed, toe clipped for individual identification, and housed in groups of four by sex. All offspring of HR families were kept, but for each C family only a random subsample of two males and two females was kept. At weaning, families were arbitrarily assigned to one of three wheel-running measurement batches such that each batch contained approximately 200 mice from nearly equal numbers of families from each line.

Probability calculations

Considering how lines were established (see above), it is very unlikely that they significantly differed in V_A at generation 0. Nevertheless, let's assume that 4 of the 8 lines had significantly lower V_A and calculate the probability that they all ended up in the selection group (see figure S5 above). We used two methods to calculate this probability, both of which yield the same answer ($P = 0.014$). The first method is based on simple probability calculation. The total number of ways to assign 4 of the 8 lines to each selection group is:

$$\binom{8}{4}$$

which is equal to 70. Assuming that 4 of the 8 lines have high V_A and 4 of 8 lines have low V_A, the number of ways of assigning all 4 low V_A lines to the HR selection group is

$$\binom{4}{4}$$

which is equal to 1, i.e., there is only one way in which all 4 low V_A lines can be assigned to the HR selection group. Thus, the probability of observing, by chance alone, 4 HR lines with low V_A is:

$$P = \frac{\binom{4}{4}}{\binom{8}{4}} = \frac{1}{70} = 0.014$$

The second method is based on simulation. The code below can be pasted directly into R, to show that the probability of observing, by chance alone, 4 HR lines with low V_A and 0 HR lines with high V_A is $P = 0.014$.

```
#################      SIMULATION START      ####################
rm(list = ls())
set.seed(101)

# Do lines end up having high genetic variance: TRUE or FALSE
hiVar <- rep(c(TRUE, FALSE), each = 4)

calcFun <- function(...){
   # randomly select 4 out of 8 lines to be in the same group -
   # so the first 4 are one group
   draw <- hiVar[sample.int(8)][1:4]
   # Now, are those 4 lines ALL the high genetic variance lines
   # (value == TRUE)

   ## Tests the condition (one-tailed test) that:
   ## all C lines VA > HR line VA

   all(draw == TRUE)
 }

N <- 1000000
system.time(obs <- replicate(N, expr = calcFun()))
mean(obs)
#################      SIMULATION END      ####################
```

Appendix S2: Genetic covariance tensor

To illustrate how the genetic covariance tensor (Hine *et al.*, 2009. Philos Trans R Soc Lond B 364:1567-1578) is applied within a Bayesian framework (Aguirre *et al*., 2014. Heredity 112:21-29), we simulated **G** matrices that differ in contrasting ways among populations. The R code below simulates 3 traits in two sets of 4 populations, with 4,600 individuals in each population. This code was used to create the datasets used to estimate **G** matrices shown in figure S8. In the first scenario (populations #1a, 1b, 1c, and 1d), the **G** matrices gradually differ among populations by a proportional amount (i.e., all elements of the matrix are changed by a constant value from population 1a through population 1d). In the second scenario (populations #2a, 2b, 2c, and 2d), **G** matrices gradually differ among populations but more for some pairs of traits than others (i.e., the top-left "corner" of the matrix is very similar among populations, but the lower-right "corner" grows more and more different among populations):

```
#############################################################################################
########################  SIMULATIONS   START ###################################
#############################################################################################
rm(list = ls())
library(nadiv)
set.seed(100)

# number of traits:
t <- 3

#Because scaled (co)variances are easier to interpret/think about, we define
an 'H matrix' which contains heritabilities along the diagonal and
correlations on the off-diagonal. By first specifying a desired total
phenotypic variance for each trait, the additive genetic and environmental
covariances (G and E matrices, respectively) are easily calculated from the H
matrix.
#The first population H matrix for both scenario 1 and 2:
##heritability on the diagonal and genetic correlation on off-diagonal
H1a <- H2a <- matrix(c(0.6, 0.25, 0.25,
                       0.25, 0.6, 0.25,
                       0.25, 0.25, 0.6), t, t, byrow = TRUE)

#Now the other populations in scenario 1, creating proportional differences:
H1b <- 0.75 * H1a
H1c <- 0.50 * H1a
H1d <- 0.25 * H1a
```

```
#Now the other populations in scenario 2, creating gradual differences:
H2b <- matrix(c(0.6, 0.18, 0.14,
                0.18, 0.4, 0.2,
                0.14, 0.2, 0.2), t, t, byrow = TRUE)
H2c <- matrix(c(0.6, 0.16, 0.098,
                0.16, 0.3, 0.07,
                0.098, 0.07, 0.15), t, t, byrow = TRUE)
H2d <- matrix(c(0.6, 0.14, 0.06,
                0.14, 0.2, 0.04,
                0.06, 0.04, 0.05), t, t, byrow = TRUE)

# Store all of these in an array:
Harray <- array(data = c(H1a, H1b, H1c, H1d, H2a, H2b, H2c, H2d),
      dim = c(t, t, 8))

# Start with each trait and population having roughly the same phenotypic
variance of 1:
P <- diag(1, t, t)

# Fill in the diagonal elements of G for each population:
Garray <- sapply(seq(dim(Harray)[3]), FUN =
function(i){diag(diag(Harray[,,i]) * diag(P), t, t)}, simplify = "array")

# Fill in the diagonal elements of the environmental (co)variance matrix for
each population. Since P=G+E, then E=P-G:
Earray <- sapply(seq(dim(Harray)[3]), FUN = function(i){diag(diag(P) -
diag(Garray[,,i]), t, t)}, simplify = "array")

# Create and fill the diagonal for phenotypic (co)variance matrices of each
population:
Parray <- Garray + Earray

# Now, fill in the off-diagonal elements of the G, E, and P matrices
for(i in 1:dim(Harray)[3]){
  for(r in 1:dim(Harray)[1]){
     if(r != dim(Harray)[1]){
        for(c in (r+1):dim(Harray)[2]){
           Garray[r, c, i] <- Garray[c, r, i] <- Harray[r, c, i] *
sqrt(Garray[r, r, i] * Garray[c, c, i])
           Parray[r, c, i] <- Parray[c, r, i] <- Harray[c, r, i] *
sqrt(Parray[r, r, i] * Parray[c, c, i])
           Earray[r, c, i] <- Earray[c, r, i] <- Parray[r, c, i] - Garray[r,
c, i]
        }
     }
  }
}

# Create a pedigree
## HS pedigree with 100 sires, 5 dams per sire, and 8 offspring per dam =
4600 individuals (2 generations):
n <- 4600

# Create array to store all of the data:
Darray <- array(dim = c(n, 13, dim(Harray)[3]))
D <- lapply(seq(dim(Darray)[3]), FUN = function(i)
as.data.frame(Darray[,,i]))
```

```
# Create an Identity matrix for the population (so don't have to do it
repeatedly below):
I <- Diagonal(n, 1)

# For each population, create breeding values and residuals for each trait
according to the G and E covariance matrices, respectively:
for(j in 1:length(D)){
   D[[j]][, 1:4] <- simPedHS(s = 100, d = 5, n = 8, uniqueDname = TRUE,
   prefix = j)
   A <- makeA(D[[j]][ ,1:3])
         D[[j]][, 5:7] <- grfx(n, G = Garray[,,j], incidence = A, output =
      "matrix")   # Breeding values
   D[[j]][, 8:10] <- grfx(n, G = Earray[,,j], incidence = I, output =
   "matrix")       # residual deviations
   D[[j]][, 11:13] <- matrix(rnorm(3, 0, 0.1), nrow = n, ncol = 3, byrow =
   TRUE) + D[[j]][, 5:7] + D[[j]][, 8:10]     # phenotype of each trait with
   mean ~ 0
   names(D[[j]]) <- c("id", "dam", "sire", "sex", paste0("bvt", seq(t)),
   paste0("et", seq(t)), paste0("pt", seq(t)))
   # Add 2 columns to indicate the population and scenario
   D[[j]][, "pop"] <- if(j <= 4) j else j-4
   D[[j]][, "scen"] <- if(j <= 4) 1 else 2
}

# Organise into one data frame:
MasterD <- do.call(rbind, D)
save("Harray", "Garray", "Earray", "Parray", "D", "MasterD", file =
"TensorExampleSim.RData")

#load(file = "TensorExampleSim.RData")

# To show it worked
# We can also check and get the estimated covariance among breeding values in
a population and compare that to the G matrix (note, these won't be exactly
the same due to Monte Carlo error)
cov(D[[1]][, c("bvt1", "bvt2", "bvt3")])
Garray[,,1]

# Same for environmental deviations
cov(D[[1]][, c("et1", "et2", "et3")])
Earray[,,1]

##############################################################################
#######################  SIMULATIONS   END ###################################
##############################################################################
####################  MCMCglmm MODELLING   START ############################
##############################################################################
library(MCMCglmm)
pops <- paste0(rep(seq(2), each = 4), rep(letters[1:4], 2))
# select the population to model [i is a number 1-8 (length of pops)]:
i <- 1

# Load the data and extract the 'popi' population data
load(file = "TensorExampleSim.RData")
assign("popi", eval(D[[i]]))
```

```
# Prepare for MCMCglmm
names(popi)[grepl("id", names(popi))] <- "animal"
PED.popi <- popi[, 1:3]

NITT <- 13000*100; THIN <- 10*100; BURNIN <- 3000*100
PRIOR <- list(R = list(V = diag(1/2,3), nu = 2.002),
              G = list(G1 = list(V = diag(1/2,3), nu = 2.002)))

M.popi <- MCMCglmm(cbind(pt1, pt2, pt3) ~ trait-1,
      random = ~ us(trait):animal,
      rcov = ~ us(trait):units,
      family = c("gaussian", "gaussian", "gaussian"),
      nitt = NITT, thin = THIN, burnin = BURNIN,
      pedigree = PED.popi,
      data = popi,
      prior = PRIOR)

# Now re-assign general 'popi' names to be specific for the particular
population chosen and then save
assign(paste0("pop", pops[i]), eval(popi))
assign(paste0("PED.pop", pops[i]), eval(PED.popi))
assign(paste0("M.pop", pops[i]), eval(M.popi))

save(list = c(paste0("pop", pops[i]), paste0("PED.pop", pops[i]),
paste0("M.pop", pops[i])), file = paste0("TensorExampleMod_pop", pops[i],
".RData"))

##############################################################################################
####################  MCMCglmm MODELLING   END ##############################
##############################################################################################
```

Looking at the simulated **G** matrices using heatmaps (figure S8 below), it is clear that the differences among populations #1a, 1b, 1c, and 1d are distributed throughout the matrix, whereas populations #2a, 2b, 2c, and 2d differ mostly in the lower-right corner of the matrix. This is because of the R code above, in which the diagonal elements are all equal for populations 1a, 1b, 1c, and 1d and the correlations between traits are also constant, with the only difference among populations are that the expected elements in H1b-d are 2/3, 1/2, and 1/3 the corresponding elements in H1a. For population #2a, 2b, 2c, and 2d, the R code above simulated substantial variation across the 4 **G** matrices in the lower-right corner, but not for elements in the top-left corner.

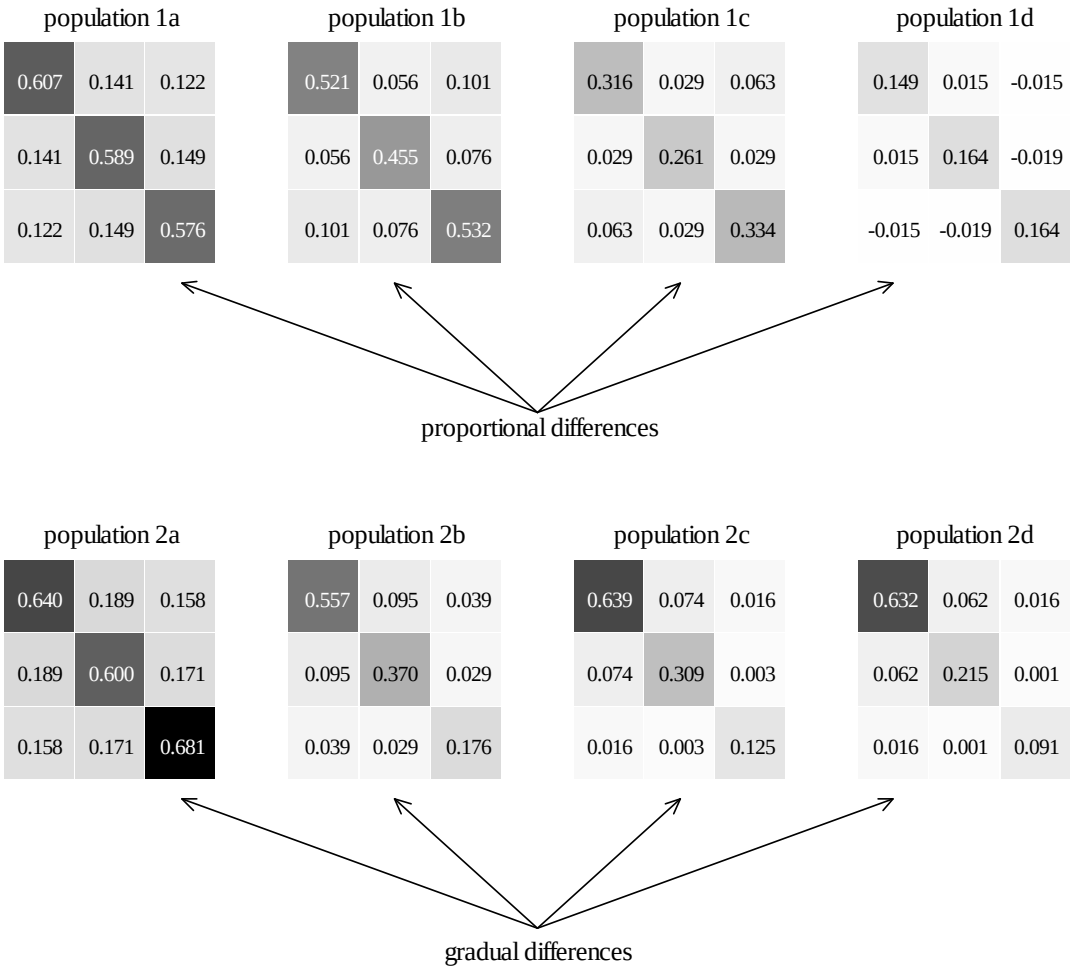

Figure S8. The estimated additive-genetic variance-covariance matrices (**G**) in the 8 simulated populations. Shown are the posterior modes from Bayesian multivariate animal models fitted with MCMCglmm (see example code above). For each **G**, the main diagonal represents the additive-genetic variance (V_A) and the off-diagonals represent the additive-genetic covariances (COV_A) for pairs of traits. The cells of the matrix are shaded according to its value (darker cell = higher V_A or COV_A), using the function "image()" in R.

We ran the code from Aguirre *et al*. (2014. Heredity 112:21-29) on these two sets of simulated **G** matrices. The covariance tensor results match what one would conclude from visually inspecting the patterns in heatmaps depicting the estimates of **G** (figure S8 above) or the expectations in the heritability matrices (R code above, H1a-d or H2a-d). For populations 1a, 1b, 1c, and 1d, the diagonal elements are all equal within each population and the correlations between traits are also constant. The only difference among populations are that the expected elements in H1b-d are 2/3, 1/2, and 1/3 the corresponding elements in H1a. The covariance tensor results reflect this, as the eigentensor $\mathbf{E}_1$ described 93.9% of the variation among the 4 **G** matrices (table S5*a*). The 95% highest posterior density (HPD) intervals of α for the nonzero eigenvalues of the genetic covariance tensor suggested that only $\mathbf{E}_1$ described significant variation among the 4 **G** matrices (figure S9*a*). As expected, $\mathbf{E}_1$ describes changes that were proportional because the variation across the 4 **G** matrices was substantial for all elements (figure S9*b*). The leading eigenvector $\boldsymbol{e}_{11}$ explained 72.9% of the variation captured by $\mathbf{E}_1$ (table S5*a*). Thus, most of the variation among the 4 **G** matrices is captured by a single combination of traits. The trait loadings of $\boldsymbol{e}_{11}$ are all roughly equal (table S5*a*); thus the 3 traits contribute roughly equally to the major axis of variation among **G** matrices. Calculating the V_A along this axis of variation shows that the changes captured in $\boldsymbol{e}_{11}$ were driven by the progressive decrease in V_A from population 1a (most V_A) to population 2d (least V_A) (figure S9*c*). This helps understanding results from the selected experiment, because it is obvious from figure 2*b* that $\mathbf{E}_1$ describes changes that were mostly proportional, that all 6 traits contributed to the major axis of variation among **G** matrices (table 1), and that selected mice harbour lower V_A along this direction ($\boldsymbol{e}_{11}$) than control mice (figure 2*c*).

Table S7. Summary of the genetic covariance tensor applied to (*a*) simulated populations #1a, 1b, 1c, and 1d, and (*b*) simulated populations 2a, 2b, 2c, and 2d. Shown are the eigenvectors (***e***; ordered by rows in terms of the absolute value) of each eigentensor (**E**), their eigenvalues, and the percent of variation they explain within their respective **E**, and loadings on each trait.

Eigentensors (**E**)	Eigenvalues of **E**	% of total variation explained	Eigenvectors (***e***) of **E**	Eigenvalues of ***e***	% of variation explained in **E**	Trait loadings		
						trait 1	trait 2	trait 3
(*a*) populations 1a, 1b, 1c, and 1d								
$\mathbf{E}_1$	0.1304	93.9%	$e_{1.1}$	-0.854	72.9%	0.579	0.574	0.579
			$e_{1.2}$	-0.415	17.2%	0.799	-0.541	-0.263
			$e_{1.3}$	-0.315	9.9%	-0.163	-0.615	0.772
$\mathbf{E}_2$	0.0035	2.5%	$e_{2.1}$	0.713	50.8%	0.461	0.887	-0.010
			$e_{2.2}$	-0.655	42.9%	0.590	-0.298	0.751
			$e_{2.3}$	-0.252	6.4%	-0.663	0.352	0.660
$\mathbf{E}_3$	0.0020	1.4%	$e_{3.1}$	0.729	53.1%	0.544	-0.678	-0.494
			$e_{3.2}$	-0.581	33.8%	0.812	0.278	0.513
			$e_{3.3}$	0.362	13.1%	-0.210	-0.681	0.702
$\mathbf{E}_4$	0.0013	0.9%	$e_{4.1}$	0.707	49.9%	0.971	0.123	-0.203
			$e_{4.2}$	-0.640	40.9%	-0.097	-0.572	-0.814
			$e_{4.3}$	0.302	9.1%	0.216	-0.811	0.544
$\mathbf{E}_5$	0.0009	0.3%	$e_{5.1}$	-0.835	69.8%	0.013	-0.640	0.768
			$e_{5.2}$	0.547	30.0%	0.850	-0.397	-0.346
			$e_{5.3}$	0.049	0.2%	-0.526	-0.658	-0.539
$\mathbf{E}_6$	0.0008	0.6%	$e_{6.1}$	0.724	52.5%	-0.563	-0.137	0.815
			$e_{6.2}$	-0.689	47.5%	-0.478	0.858	-0.186
			$e_{6.3}$	0.012	0.0%	0.674	0.494	0.549
(*b*) populations 2a, 2b, 2c, and 2d								
$\mathbf{E}_1$	0.1309	93.3%	$e_{1.1}$	-0.952	90.6%	-0.276	-0.466	-0.841
			$e_{1.2}$	-0.296	8.8%	-0.102	-0.856	0.508
			$e_{1.3}$	0.077	0.6%	0.956	-0.226	-0.188
$\mathbf{E}_2$	0.0041	2.9%	$e_{2.1}$	0.805	64.8%	0.959	-0.006	0.284
			$e_{2.2}$	-0.578	33.4%	0.031	0.996	-0.081
			$e_{2.3}$	0.134	1.8%	-0.282	0.086	0.955
$\mathbf{E}_3$	0.0022	1.6%	$e_{3.1}$	0.886	78.6%	0.741	0.646	-0.183
			$e_{3.2}$	0.355	12.6%	0.647	-0.760	-0.064
			$e_{3.3}$	-0.297	8.8%	0.181	0.072	0.981
$\mathbf{E}_4$	0.0015	1.1%	$e_{4.1}$	0.785	61.6%	0.700	-0.473	-0.535
			$e_{4.2}$	-0.463	21.4%	-0.694	-0.625	-0.356
			$e_{4.3}$	0.412	17.0%	0.167	-0.621	0.766
$\mathbf{E}_5$	0.0009	0.6%	$e_{5.1}$	-0.743	55.2%	0.649	-0.697	0.305
			$e_{5.2}$	0.663	43.9%	0.586	0.202	-0.785
			$e_{5.3}$	-0.093	0.9%	0.485	0.688	0.540
$\mathbf{E}_6$	0.0008	0.5%	$e_{6.1}$	-0.798	63.7%	-0.081	0.609	-0.789
			$e_{6.2}$	0.602	36.2%	0.337	-0.729	-0.596
			$e_{6.3}$	0.005	0.0%	0.938	0.314	0.146

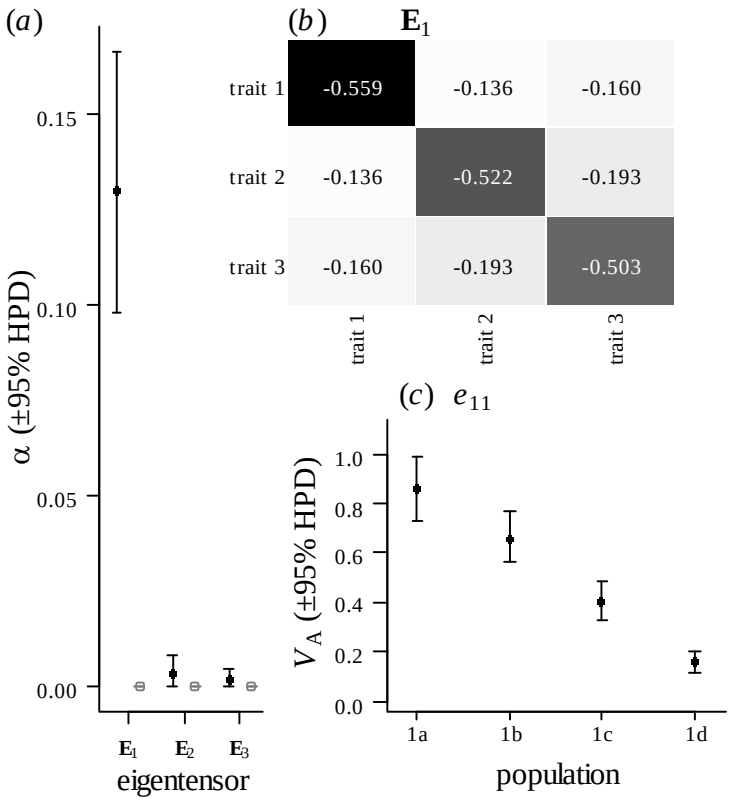

Figure S9. The genetic covariance tensor approach applied to simulated **G** matrices from fictive populations #1a, 1b, 1c, and 1d. (*a*) Variance [α; ±95% highest posterior density (HPD) intervals] accounted for by each eigentensor ($\mathbf{E}_n$) for the observed (black dots) and randomized (i.e., null hypothesis; grey dots) sets of **G**. Because the 95% HPD intervals of the observed vs. randomized sets of **G**s did not overlap for $\mathbf{E}_1$, this eigentensor described significantly more variation among the observed **G** than by chance. (*b*) "Heat map" displaying the pattern of greatest variation among **G** matrices as captured by $\mathbf{E}_1$ (darker shading indicates more variation among **G** matrices). As expected, variability among **G** matrices is distributed throughout the entire matrix. (*c*) Across populations, the additive-genetic variance (V_A) in the direction of the first eigenvector of $\mathbf{E}_1$ (i.e., $\boldsymbol{e}_{11}$).

We can also inspect the patterns from heatmaps depicting the estimates of **G** (figure S8 above) or the heritability matrices in the code for populations 2a, 2b, 2c, and 2d (see H2a-d in R code above). In this second scenario, the four **G** matrices gradually change from the top-left corner being fairly similar among populations to the bottom-right corner being very different among populations. In the covariance tensor analysis, the eigentensor $\mathbf{E}_1$ described 93.3% of the variation among the 4 **G** matrices (table S5*b*). The 95% HPD intervals of α for the nonzero eigenvalues of the genetic covariance tensor suggested that only $\mathbf{E}_1$ described significant variation among the 4 **G** matrices (figure S10*a*). As expected, $\mathbf{E}_1$ describes changes that were gradually distributed throughout the matrix because the variation across the 4 **G** matrices was substantial for elements in the lower-right corner, but not for elements in the top-left corner (figure S10*b*). The leading eigenvector $\boldsymbol{e}_{11}$ explained 90.6% of the variation captured by $\mathbf{E}_1$ (table S5*b*). The trait loadings of $\boldsymbol{e}_{11}$ (table S5*b*) for traits 1, 2, and 3 are -0.276, -0.466, and -0.841, suggesting that they respectively contribute slightly, moderately, and strongly to the major axis of variation among **G** matrices. Calculating the V_A along this axis of variation shows that the changes captured in $\boldsymbol{e}_{11}$ were driven by a gradual decrease in V_A from population 2a (most V_A) to population 2d (least V_A) (figure S10*c*). Again, this helps understanding results from the selected experiment, because in figure 2*b* we can see that $\mathbf{E}_1$ describes changes that were most intense in the lower-right corner of the **G** matrix (the area under most intense selection).

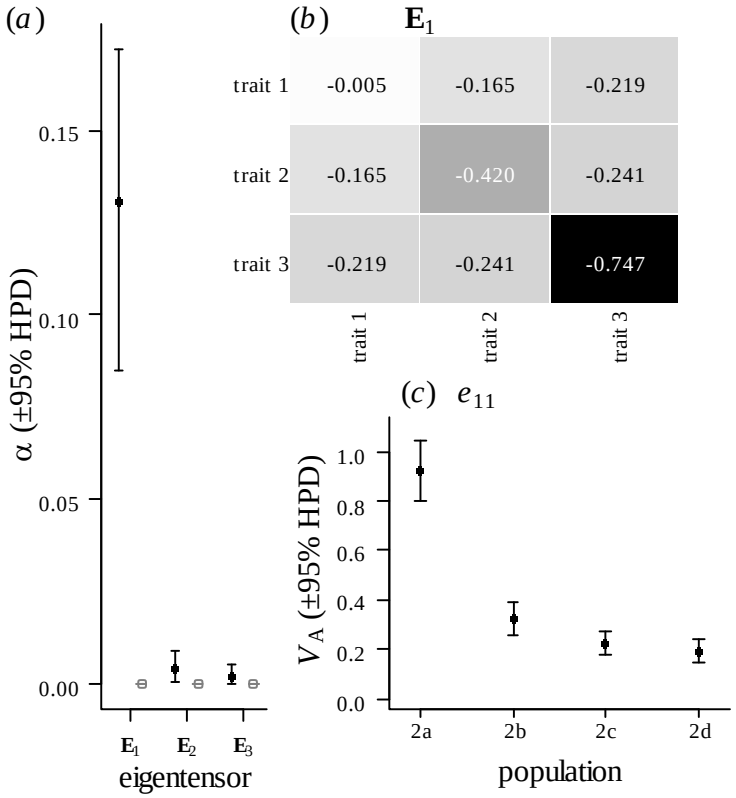

Figure S10. The genetic covariance tensor approach applied to simulated **G** matrices from fictive populations 2a, 2b, 2c, and 2d. (*a*) Variance [α; ±95% highest posterior density (HPD) intervals] accounted for by each eigentensor ($\mathbf{E}_n$) for the observed (black dots) and randomized (i.e., null hypothesis; grey dots) sets of **G**. Because the 95% HPD intervals of the observed vs. randomized sets of **G**s did not overlap for $\mathbf{E}_1$, this eigentensor described significantly more variation among the observed **G** than by chance. (*b*) "Heat map" displaying the pattern of greatest variation among **G** matrices as captured by $\mathbf{E}_1$ (darker shading indicates more variation among **G** matrices). As expected, variability among **G** matrices is more intense in the lower-right corner of the matrix. (*c*) Across populations, the additive-genetic variance (V_A) in the direction of the first eigenvector of $\mathbf{E}_1$ (i.e., $\boldsymbol{e}_{11}$).